Journal of Current Science and Technology, January-April 2021 Vol. 11 No. 1, pp. 1-14

ISSN 2630-0656 (Online)

Cite this article: Emudom, V., & Suyabodha, A. (2021, January). The studies on the use of magnetic particle suspensions for heat transfer enhancement in vertical pipe flow. *Journal of Current Science and Technology, 11*(1), 1-14. DOI: 10.14456/jcst.2021.3

Journal of Current Science and Technology

Journal homepage: https://jcst.rsu.ac.th

The studies on the use of magnetic particle suspensions for heat transfer enhancement in vertical pipe flow

Varut Emudom[1*] and Apiwat Suyabodha[2]

[1]Department of Mechanical Engineering, College of Engineering, Rangsit University, Patumthani 12000, Thailand
[2]Department of Automotive Engineering, College of Engineering, Rangsit University, Patumthani 12000, Thailand

[*]Corresponding author; E-mail: varutama8008@gmail.com

Received 16 June 2020; Revised 31 July 2020; Accepted 25 September 2020;
Published online: 30 January 2021

Abstract

This paper presents an experimental study of the heat transfer enhancement of magnetic particle suspensions consisting of magnetic particles (gamma-typed iron oxides, Fe_2O_3) (10-15 nm) and distilled water. The experiments were carried out at different volume concentrations (ϕ) of 0.5%, 1.0%, 1.5%, and 2.0% in a vertical pipe flow. Five different intensities (0G, 600 G, 1200 G, 1800 G, and 2400 G) of the external magnetic field were applied during pipe flow to enhance the heat transfer. The location of the solenoid coils (60 mm and 120 mm separation between the coils) for an externally applied magnetic field was also tested to study its effect on heat transfer performance. All tests were in between high laminar regime and low turbulent regime (2800-9760). The uniform surface heat flux is directly imposed along the surface area of the copper tube during heat transfer experiments. The results showed that, as the magnetic particle concentration and intensity of the external magnetic field increased, the local heat transfer coefficient increased. The maximum heat transfer enhancement of 19% as compared to the base case (0G) can be attained at particle volume concentration of 2.0% and external magnetic field with the strength of 2400 G. The heat transfer enhancement decreased with the increasing of distance between solenoid coils. Hence, the effect of external magnetic field on decreasing the temperature along the tube section is more desirable as the distance of the coils remains closer to each other.

Keywords: *heat transfer coefficient, heat transfer enhancement, magnetic field, solenoid coils, surface heat flux, vertical pipe flow*

1. Introduction

Conventional heat transfer fluids such as water and oil with low thermal conductivity have limitations on improving the performance efficiency of many pieces of engineering equipment. To improve engineering equipment such as heat exchangers and all kinds of electronic devices, many attempts have been accomplished to substitute the use of heat transfer fluids with higher thermal conductivity. An innovative attempt for enhancing the thermal conductivity of the fluids is the use of very small magnetic particles as the dispersed phase. The magnetic particles must have an average size range under 50 nm to be able to uniformly and stably be suspended in a liquid. Energy transport of the magnetic particle suspensions is also affected by the solid volume concentration. A number of recent experiments have indicated dramatic improvements in effective thermal conductivity (Jeong, Kwon, Lee, Kim, & Yun, 2013; Esfe, Afrand, Karimipour, Yan, & Sina, 2015). The thermal conductivity ratio of magnetic particle suspensions with respect to pure water can be increased with the increase of the strength of the applied magnetic field (Karimi, Goharkhah, Ashjaee, & Shafii, 2015). Another researcher reported that the thermal conductivity of magnetic particle suspensions increases exponentially with particle volume concentration and temperature of the suspension (Hojjat, Etemad, Bagheri & Thibault, 2011). There are few publications on the heat transfer performance of magnetic particle suspensions in the vertical pipe flow. To apply the magnetic particles to practical heat transfer processes, more studies on its flow are needed.

Magnetic particle suspensions consist of a nonmagnetic carrier fluid and ferromagnetic particles as a dispersed phase (Zhou, Gu, Meng, & Shao, 2019). The magnetic particles are typically very small in the range of 10-50 nm in diameter, which are coated with surfactant layers to keep them stably suspended in a carrier fluid (Liou, Wei, & Wang, 2019). However, some magnetic particles may aggregate as the result of dipole-dipole interactions (Khodadadi, Toghraie, & Karimipour, 2019). In the absence of the externally applied magnetic field, the magnetic particles are randomly oriented and the suspension has no net magnetization. When imposed by the external magnetic field, the magnetic particles in the suspension align to form chain-like structures in the direction of the magnetic field (Arabpour, Karimipour, & Toghraie, 2018). The magnetic particle suspensions have potential for many applications in heat transfer because they can be controlled by the strength of the externally applied magnetic field and temperature variation. Bahiraei and Hangi (2015) reviewed some of the characteristics of heat transfer in magnetic fluids. An experimental investigation to determine the viscosity of magnetic particle suspensions to be applied for heating and cooling systems was reported by Toghraie, Alempour, and Afrand (2016). Some dispersants such as gum acaria, sodium dodecyle benzene sulfonate (SDBS) and cetyl trimethyl ammonium chloride were studied to improve high stability of the suspensions, hence, increase heat transfer performance (Sun, Lei, & Yang, 2015). An interesting report to determine the effects of a constant and oscillating applied magnetic field on heat transfer enhancement was investigated. The local heat transfer coefficient varies with the frequency of the oscillating applied field (Yarahmadi, Goudarzi, & Shafii, 2015). The effects of the magnetic field induced by a finite length solenoid on the forced convection heat transfer in a pipe partially filled with porous medium were investigated (Fadaei, Shahrokhi, Dehkordi, & Abbasi, 2019). The combined effects of the magnetic field and the porous medium can result in a higher mixing intensity and breakage of the thermal boundary layer which in turn optimizes the enhancement of the local heat transfer coefficients and local Nusselt number values. Many numerical investigations were also conducted to determine heat transfer characteristics of the magnetic particle suspensions. Models such as a zigzag-shaped microchannel (Toghraie, Abdollah, Pourfattah, Akbari, & Ruhani, 2018) and a channel with sinusoidal walls (Rashidi, Nasiri, Khezerloo, & Laraqi, 2016) were used. The studies showed that the increase in heat transfer can be obtained in the sinusoidal microchannel without using any magnetic particles. The local heat transfer coefficient can be increased by decreasing the wavelengths of sinusoidal and zigzag-shaped microchannels. An experimental investigation of two-phase closed thermosiphon filled with nanofluids was carried out to investigate some applications such as electronic cooling (Sardarabadi, Heris, Ahmadpour, & Passandideh-Fard, 2019). The algorithms and architectures were developed by using ANNs to measure thermal conductivity and viscosity of nanofluids suitable for many sensitivity cases (Shahsavar, Khanmohannadi, Toghraie, & Salihepour, 2019).

In this paper, the heat transfer performance of magnetic particle suspensions was investigated in the vertical pipe flow experiments. The objective was to find important parameters such as the particle volume concentrations, the intensity and the location of external applied magnetic fields which can optimize the enhancement of heat transfer by magnetic particle suspensions.

2. Objectives

The objective of this study is to demonstrate important parameters such as the particle volume concentrations, the intensities of external magnetic field and the location of magnetic coils which have major effects on heat transfer enhancement in vertical pipe flow. The heat transfer enhancement can be maximized with high particle volume concentration and intensity of the externally applied magnetic field. The heat transfer enhancement is also more considerable when the distance of the coils remains closer to each other.

3. Materials and methods

3.1 Apparatus

A schematic of heat transfer experiments in vertical pipe flow is shown in Figure 1.

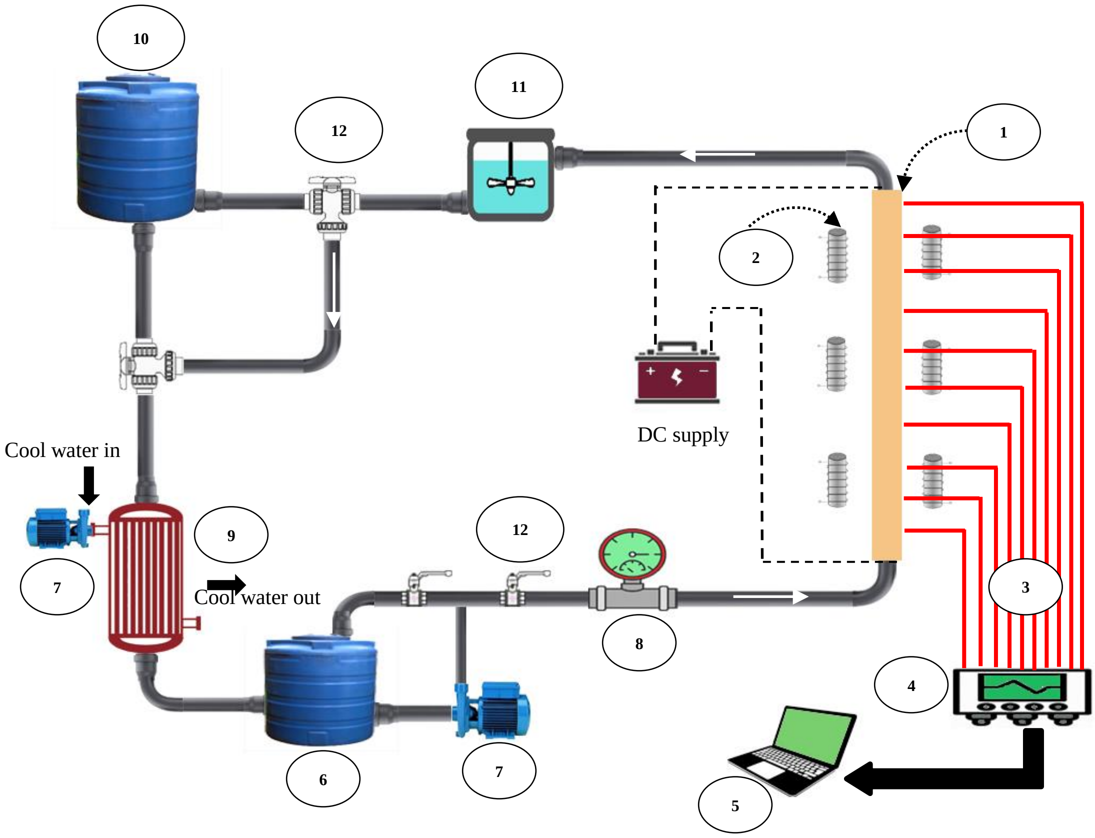

1	Copper tube	5	Computer	9	Heat exchanger
2	Solenoid coils	6	Reservoir tank	10	Overhead reservoir
3	Thermocouple wires	7	Pump	11	Separator
4	Data logger	8	Flow meter	12	Control valve

Figure 1 Schematic diagram of the experimental apparatus

The experimental system consisted of a flow loop, a heated test section, a heat exchanger, pumps, solenoid coils, measuring and control units. Ten thermocouples were connected to the surface of copper tube to measure the wall temperature at different locations. By its cooling effect, the heat exchanger was used to keep a constant temperature of the magnetic particle suspensions at an inlet of the test section. Three pairs of solenoid coils were placed at the right and left side of test section to apply the external magnetic field. A magnetic field with a magnitude of up to 2400 G along a test section was very complicated to construct. Six separated solenoid coils which were coupled with each other were considered where the distance between them could be adjusted. The DC power supplier with a maximum current of 50 Amp and maximum voltage of 150 V was used to produce the magnetic field. The direction of the external magnetic field was perpendicular to the axial flow direction of the magnetic particle suspensions. The magnetic field strength was measured by a Gauss meter. The cross section of test section is shown explicitly in Figure 2.

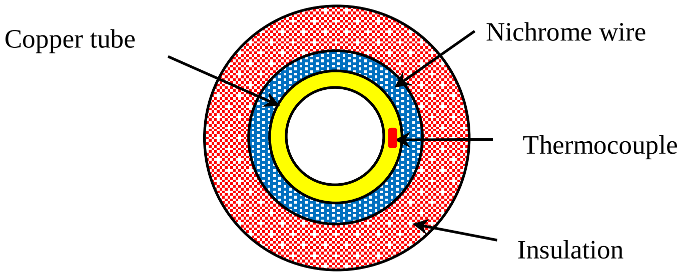

Figure 2 Cross section of the test tube

The test section included a straight copper tube with 850 mm length, 15 mm inner diameter and 20 mm outer diameter. To impose uniform surface heat flux, the copper tube was wrapped by the Nichrome wire which was then connected to a DC supply with maximum power of 500 W. Insulation such as aluminum foil and rubber were wrapped on the outer surface of the test section to minimize the heat transfer loss. With respect to the tube inlet, the thermocouples number 1 to 10 were placed at these distances: 45 mm, 180 mm, 230 mm, 315 mm, 400 mm, 450 mm, 535 mm, 620 mm, 670 mm, and 750 mm. To study the effects of solenoid coils' placement, three pairs of solenoid coils were located at the distance of 60 mm apart and 120 mm apart. For 60 mm separation between three pairs, the thermocouple numbers 2, 3, 5, and 7 were directly influenced by the external magnetic field. For 120 mm of separated distance between three pairs, the thermocouple numbers 2, 3, 5, 6, 8, and 9 were directly influenced by the external magnetic field.

3.2 Materials and preparation

The magnetic particle suspensions used in this study were composed of magnetic particles in the form of gamma-typed iron oxides Fe_2O_3 and distilled water. The Fe_2O_3 iron oxides are ferromagnetic materials known for their cubic cell structures and the moments of the individual atoms are aligned in the same direction (Bahiraei, & Hangi, 2015). The particles have magnetic permeability constants in the range of 0.5-35.5 and average size diameters of 10-15 nm (Rosensweig, 1997). Thermal agitation or Brownian motion (kT, where k is Boltzman's constant and T is an absolute temperature) helps to disperse magnetic particles in the water. The dipole-dipole contact energy, E_{dd} is the energy required to break a bond between two magnetic particles (Rosensweig, 1997).

$$E_{dd} = \frac{\mu_0 M^{2/3} V}{12} \quad (1)$$

The permeability of free space (μ_0) has the value of $4\pi \times 10^{-7}$ H/m. M is the intensity of magnetization and V is the volume of a dipole. In order to escape the agglomeration between two magnetic particles, it is necessary for the thermal agitation to exceed the dipole-dipole contact energy. We define γ as the ratio of these two quantities (Rosensweig, 1997).

$$\gamma = \frac{E_{dd}}{kT} = \frac{\mu_0 M^{2/3} V}{12kT} \quad (2)$$

The ratio is kept as low as possible. In this experiment the ratio of γ is calculated to be less than 0.0001. Additionally, the diameter of magnetic particles is also important. In order to keep a stable suspension of magnetic particles in the water, Rosensweig (1997) claimed that the average magnetic particle diameter (d) must be expressed by

$$d \le \left(\frac{144kT}{\pi \mu_0 M^2}\right)^{1/3} \quad (3)$$

For this study, the average magnetic particle size was 10 nm-15 nm which satisfied the above condition. To prepare for magnetic particle suspensions, ultrasonication was used to disperse magnetic particles in distilled water. The magnetic particles were ultrasonicated for 30 min to break up any agglomerations or clusters in the dry powder form before running the experiments. The magnetic particle suspensions were then rested at room temperature for 2 hours after ultrasonication to reduce any heating effects. The volume concentrations of magnetic particles were tested at 0.5%, 1.0%, 1.5%, and 2.0%.

3.3 Analysis of data

From Newton's law of cooling, the local heat transfer coefficient can be calculated as follows

$$h(y) = \frac{q_s''}{T_s(y) - T_m(y)} \tag{4}$$

where q_s'' is the uniform surface heat flux which was imposed on the copper tube in the test section. T_s is the surface or wall temperature along the copper tube. T_m is the mean temperature of the suspensions. We used y as the vertical coordinate which initiated at y = 0, the copper tube inlet. In a thermally fully developed region, for uniform surface heat flux, Incropera and DeWitt (1996) stated that

$$\left(\frac{dT_s}{dy}\right)_{fd,t} = \left(\frac{dT_m}{dy}\right)_{fd,t} \tag{5}$$

For the entire tube, Incropera and DeWitt (1996) expressed that the total tube heat transfer rate can be calculated as the following equation

$$q_{conv} = \dot{m}c_p(T_{m,exit} - T_{m,inlet}) \tag{6}$$

where q_{conv} is the total tube heat transfer rate, $\dot{m}$ is the mass flow rate, c_p is the specific heat. Thus, from Equation (4), Incropera and DeWitt (1996) stated that the rate of change between the suspensions' mean temperature and the axial distance y can be expressed as the following equation

$$\frac{dT_m}{dy} = \frac{q_s''}{\dot{m}c_p} h(T_s - T_m) \tag{7}$$

where $P = \pi D$ is the surface perimeter for a circular tube. By integrating from y = 0 at the tube inlet, the mean temperature of the suspension can be expressed as follows

$$T_m(y) = T_{m,inlet} + q_s'' Py/\dot{m}c_p \tag{8}$$

Uniform surface heat flux, q_s'' can be expressed in terms of the supplied current and voltage as follows

$$q_s'' = \frac{Q}{A_s} = \frac{IV}{\pi DL} \tag{9}$$

where I is the measured current, V is the supplied voltage, D is the true diameter and L is the heated length.

Finally, using the obtained local convection heat transfer coefficients, the average value is then calculated by integrating local h(y) for the entire length (y = 0 to y = L) and dividing by the total length of the tube

$$h_{avg} = 1/L(\int h(y)dy) \tag{10}$$

3.4 Uncertainty analysis

Uncertainty (σ) of the experimental data may arise from the errors of some measurements. These quantities are the heat flux, the wall temperature along copper tube, the electric current, the supplied voltage, the distance between thermocouples and the distance between solenoid coils. From Equation (4), the uncertainty of the local heat transfer coefficient is calculated as follows

$$\sigma_h = \pm\sqrt{\left(\frac{\partial h}{\partial q_s''}\sigma_{q_s''}\right)^2 + \left(\frac{\partial h}{\partial T_s}\sigma_{T_s}\right)^2 + \left(\frac{\partial h}{\partial T_m}\sigma_{T_m}\right)^2} \tag{11}$$

From Equations (8) and (9), the uncertainties of the mean temperatures of the suspensions and uniform surface heat flux are calculated as follows:

$$\sigma_{T_m} = \pm\sqrt{\left(\frac{\partial T_m}{\partial T_{m,i}}\sigma_{T_{m,i}}\right)^2 + \left(\frac{\partial T_m}{\partial y}\sigma_y\right)^2} \tag{12}$$

$$\sigma_{q_s''} = \pm\sqrt{\left(\frac{\partial q_s''}{\partial I}\sigma_I\right)^2 + \left(\frac{\partial q_s''}{\partial V}\sigma_V\right)^2} \tag{13}$$

The uncertainties of the measurements in this study are summarized in Table 1.

Table 1 Uncertainty of the measurement

Quantity	Uncertainty
ΔT_s (°C)	0.2
ΔL (m)	1×10^{-3}
ΔI (Amp)	0.1
ΔV (Volt)	0.1

From Equation (10), the relative uncertainty of the local heat transfer coefficient is calculated as follows

$$U_h = \frac{\sigma_h}{h} = \pm\sqrt{\frac{1}{h^2}[(\frac{\partial h}{\partial q_s''}\sigma_{q_s''})^2 + (\frac{\partial h}{\partial T_s}\sigma_{T_s})^2 + (\frac{\partial h}{\partial T_m}\sigma_{T_m})^2]} \quad (14)$$

From Equation (12), the relative uncertainty of the surface heat flux is calculated as follow

$$U_{q_s''} = \frac{\sigma_{q_s''}}{q_s''} = \pm\sqrt{\frac{1}{q_s''^2}[(\frac{\partial q_s''}{\partial I}\sigma_I)^2 + (\frac{\partial q_s''}{\partial V}\sigma_V)^2]} \quad (15)$$

The uncertainty values have been calculated for all the measured cases. The percentage uncertainty in the calculation of the local heat transfer coefficient is $\pm 3.8\%$.

4. Results

Figures 3-6 show the effects of different intensities (0 G-2400 G) of the external applied magnetic field on the suspensions' temperature profile for particle volume concentrations of 0.5%, 1.0%, 1.5%, and 2.0%, respectively.

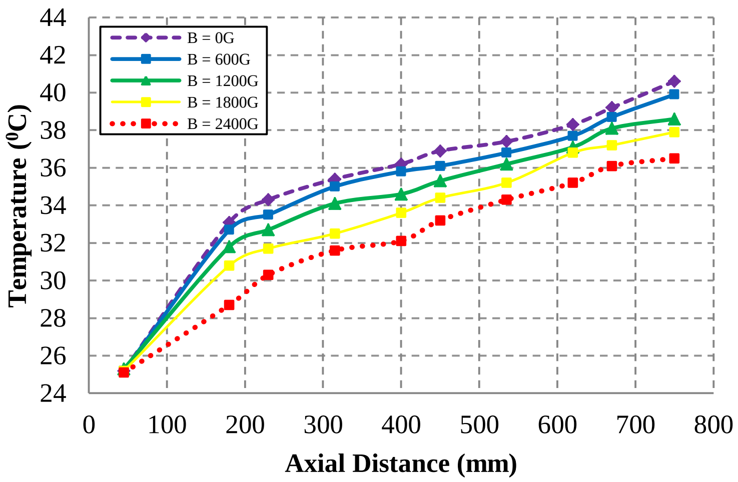

Figure 3 Effect of magnetic field on the temperature of suspension for 0.5% vol.

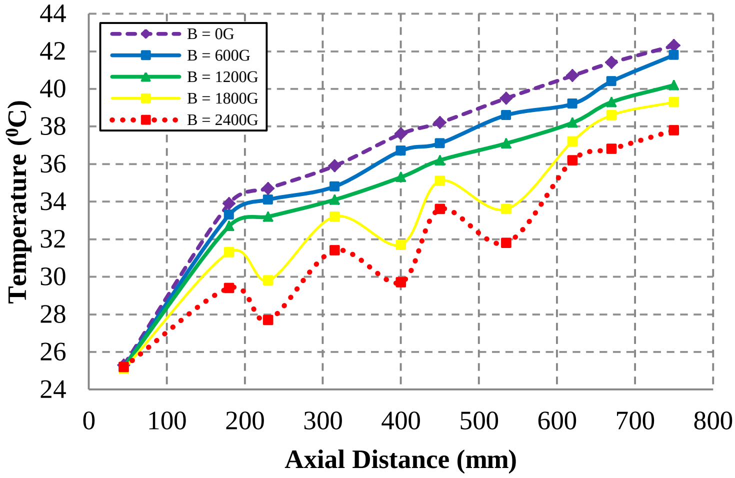

Figure 4 Effect of magnetic field on the temperature of suspension for 1.0% vol.

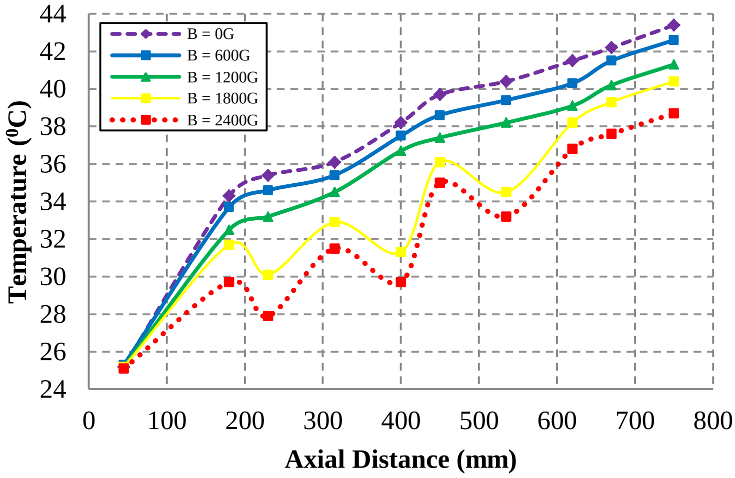

Figure 5 Effect of magnetic field on the temperature of suspension for 1.5% vol.

The constant surface heat flux was loaded over the copper tube by a Nichrome wire. The three pairs of solenoid coils used to supply the external magnetic field were placed 60 mm apart from each other. The results indicated that the temperature of the suspensions had been remarkably decreased by application of the external magnetic field to the flow of the suspensions. As the particle volume concentrations increased, the suspensions' temperature decreased significantly. The maximum temperature drop of 9^{o}C could be seen for the particle volume concentration of 2% and the external magnetic field with an intensity of 2400 G. At 60 mm separation between three pairs of solenoid coils, the thermocouple numbers 2, 3, 4, 5, and 7 were directly influenced by the external magnetic field. The significant drop in temperature at these locations could be observed especially at the high intensity of the external magnetic field.

The local heat transfer coefficients are presented in Figures 7-10 as a function of relative axial distance from the entrance of the copper tube for particle volume concentrations of 0.5%, 1.0%, 1.5%, and 2.0%, respectively.

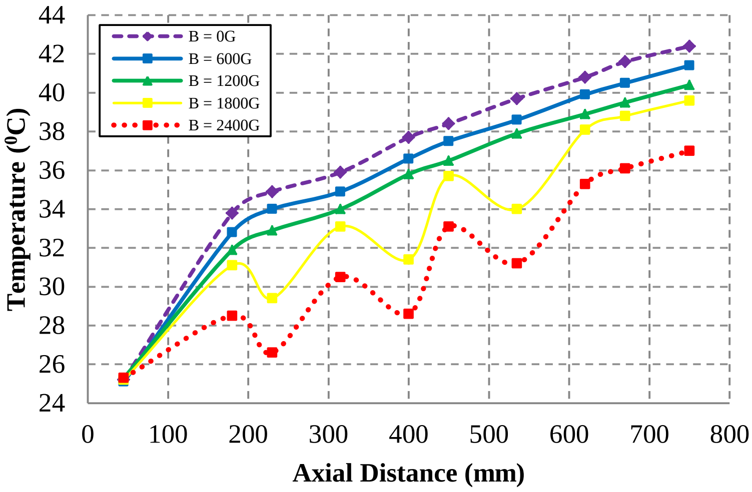

Figure 6 Effect of magnetic field on the temperature of suspension for 2.0% vol.

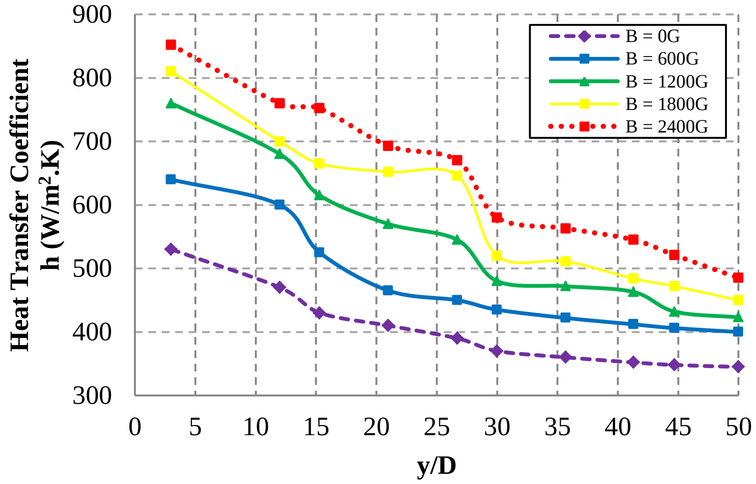

Figure 7 Profile of heat transfer coefficients for different intensities at 0.5% vol.

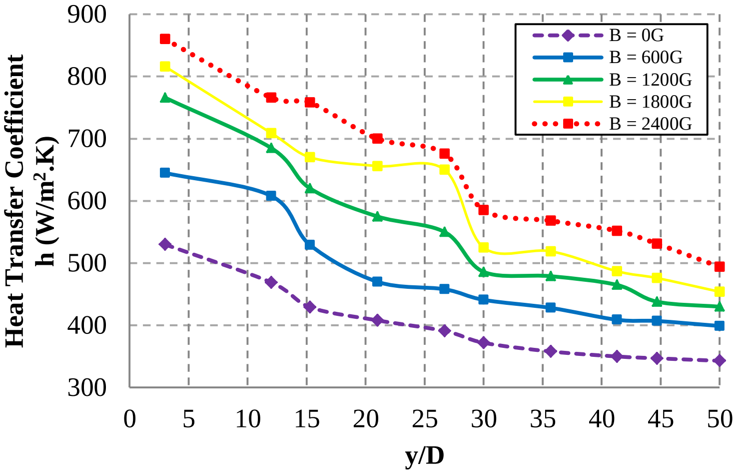

Figure 8 Profile of heat transfer coefficients for different intensities at 1.0% vol.

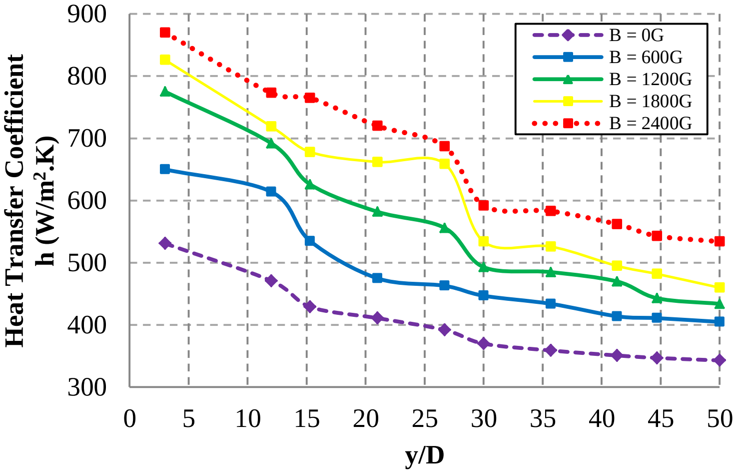

Figure 9 Profile of heat transfer coefficients for different intensities at 1.5% vol.

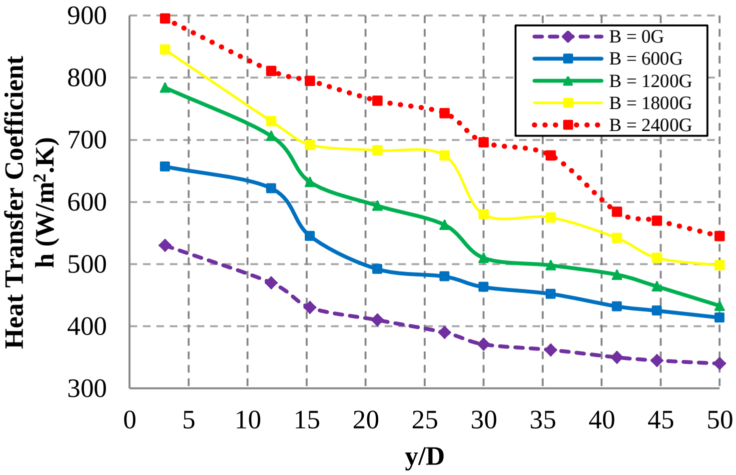

Figure 10 Profile of heat transfer coefficients for different intensities at 2.0% vol.

Some trends can be observed. Without applying an external magnetic field to the flow, the magnetic particle suspensions could not perform well in heat transfer enhancement, hence, low numbers for the local heat transfer coefficient. The local heat transfer coefficients h decreased with increasing axial distance starting from the entrance of the copper tube to the exit. As the particle volume concentrations increased, the local heat transfer coefficients also increased. By applying a stronger magnetic field, an intensive heat transfer performance could be acquired.

Figure 11 shows that using magnetic particle suspension increases the convective heat transfer. The average convective heat transfer coefficient increases as the Reynolds number and the volume concentration of magnetic particles increase. It can be inferred that increasing the volume concentration of magnetic particles leads to improvement of the convective heat transfer.

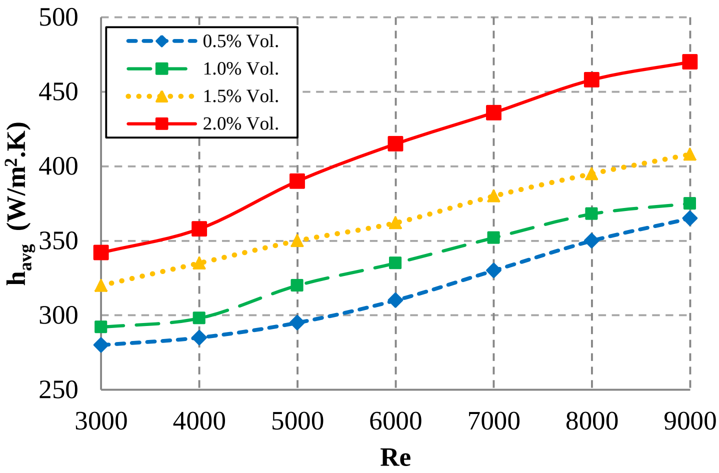

Figure 11 Average convective heat transfer coefficient as a function of the Reynolds number

In another experiment, the position of the solenoid coils was shifted in order to investigate the effect of solenoid coil location on the temperature profile. Each pair of the solenoid coils was positioned 120 mm from each other. The thermocouple numbers 2, 3, 5, 6, 8, and 9 were directly under the effect of magnetic field. Figures 12 and 13 show the trend of temperature variation along the test section for particle volume concentrations of 1.0% and 2.0%, respectively. When the coils were separated by 60 mm, the temperature drop was more considerable than when the coils were separated by 120 mm. The temperature drop under the effect of magnetic field was likely local when the position of coils became farther apart from each other. Thus, for 120 mm separation, the temperature drop could be seen locally at thermocouple numbers 2, 3, 5, 6, 8, and 9 where there was the direct influence of magnetic field.

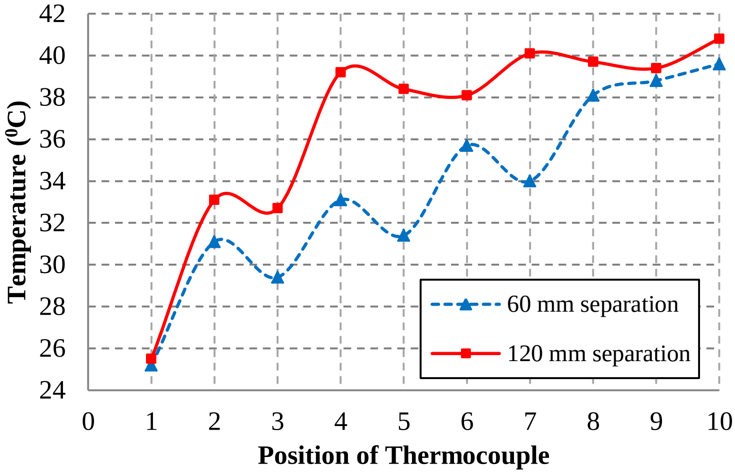

Figure 12 The effect of location of magnetic field on suspensions' temperature for 1.0% vol.

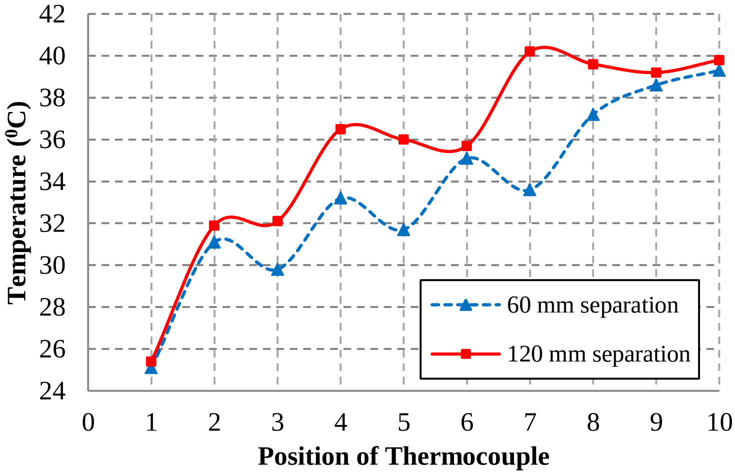

Figure 13 The effect of location of magnetic field on suspensions' temperature for 2.0% vol.

5. Discussion

There are some plausible explanations of heat transfer enhancement from this experiment. The local convective heat transfer decreases with the axial distance because of the growth of the thermal boundary layer. However, use of the magnetic particle suspension can increase the average heat transfer coefficient, therefore, the heat transfer is enhanced. It can be inferred that increasing the volume concentration of magnetic particles leads to improvement of the convective heat transfer. In the absence of an external magnetic field, the magnetic moments are oriented in random directions and magnetic particles are dominated by the Brownian motion as thermal energy exceeds the magnetic dipolar energy, E_{dd} (Esfe, Raki, Emami, & Afrand, 2019). By applying the external magnetic field to the magnetic particle suspensions, the magnetic dipolar energy becomes strong enough to dominate the thermal energy (Keyvani, Afrand, Toghraie, & Reiszadeh, 2018). The magnetic moments in the magnetic particles start to align forming doublets, triplets and short chain-like structures in the direction of magnetic field. As the strength of magnetic field increases, the magnetic particles start to form more chain-like structures. For high particle volume concentration, these linear chain-like structures become longer and can remarkably enhance the heat transfer. At lower particle volume concentration, lesser number of particles gets aligned (Meyer, Adio, Sharifpur, & Nwosu, 2016). Therefore, the heat transfer enhancement is less considerable. It is predicted that the thermal conductivity of the magnetic particle suspensions declines and the amount of temperature drop decreases as well (Zadeh, & Toghraie, 2018). The effect of a magnetic field on decreasing the temperature is much more considerable when the distance of the solenoid coils remains closer. This demonstrates that as the distance of the coils increases, the magnetic particles do not have enough time to agglomerate to form the chain-like structures. This incapability results in loss of heat absorption. Furthermore, when these chain-like structures are broken up in the pipe flow due to rotating eddies, heat is lost during this process. Thus, the formation of chain-like structures is needed quickly to absorb any heat loss. The forced convective heat transfer can be enhanced by increasing thermal conductivity of the suspensions (Hussain, Mehmood, & Sagheer, 2016). The magnetic torque which tends to align the magnetic moments of magnetic particles with the direction of the external magnetic field is known to be the mechanism of suspensions' thermal conductivity (Karimi et al., 2015). Thus, increasing the strength of the external magnetic field can increase the suspensions' thermal conductivity, hence, the significant increase in heat transfer enhancement.

Further investigations from this study can be made by rotating the direction of the external magnetic field. In this study, we only investigated the perpendicular direction of the applied magnetic field to the flow direction. An angular direction of the applied magnetic field can also play an important role in heat transfer enhancement because of factors such as the shape of chain-like structures, the rate of agglomeration formation, the rate of enhancement and the rate of reformation after the chain breakage under the effects of eddies in pipe flow.

6. Conclusion

The heat transfer enhancement of magnetic particle suspensions of gamma-typed iron oxides Fe_2O_3 with 10-15 nm particle size was experimentally investigated in a vertical heated copper tube. The use of iron oxides Fe_2O_3 magnetic particles dispersed in water cannot enhance the heat transfer in the pipe flow without the application of the external magnetic field. The enhancement of heat transfer, hence, the average heat transfer coefficient $\bar{h}$ is more significant under the influence of the external applied magnetic field. The heat transfer enhancement increases with the increasing magnetic particle volume concentrations and the magnitude of the external magnetic field. The spacing between the applied magnetic fields must remain closer to each other to maximize the heat transfer enhancement.

7. References

Arabpour, A., Karimipour, A., & Toghraie, D. (2018). The study of heat transfer and laminar flow of kerosene/multi-walled carbon nanotubes (MWCNTs) nanofluid in the microchannel heat sink with slip boundary condition. *Journal of Thermal Analysis and Calorimetry*, *131*(2), 1553-1566. DOI: 10.1007/s10973-017-6649-x

Bahiraei, M., & Hangi, M. (2015). Flow and heat transfer characteristics of magnetic nanofluids: A review. *Journal of Magnetism and Magnetic Materials*, *374*, 125-138. DOI: 10.1016/j.jmmm.2014.08.004

Esfe, M. H., Afrand, M., Karimipour, A., Yan, W. M., & Sina, M. (2015). An experimental study on thermal conductivity of MgO nanoparticles suspended in a binary mixture of water and ethylene glycol. *International Communication of Heat and Mass Transfer*, *67*, 173-175. DOI: 10.1016/j.icheatmasstransfer.2015.07.009

Esfe, M. H., Raki, H. R., Emami, M. R. S., Afrand, M. (2019). Viscosity and rheological properties of antifreeze based nanofluid containing hybrid nano-powders of MWCNTs and TiO_2 under different temperature conditions. *Powder Technology*, *342*, 808-816. DOI: 10.1016/j.powtec.2018.10.032

Fadaei, F., Shahrokhi, M., Dehkordi, A. M., & Abbasi, Z. (2019). Forced-convection heat transfer of ferrofluids in a circular duct partially filled with porous medium in the presence of magnetic field. *Journal of Magnetism and Magnetic Materials*, *475*, 304-315. DOI: 10.1016/j.jmmm.2018.11.032

Hojjat, M., Etemad, S.Gh., Bagheri, R., & Thibault, J. (2011). Thermal conductivity of non-Newtonian nanofluids: experimental data and modeling using neural network. *International Journal of Heat and Mass Transfer*, *54*(5-6), 1017-1023. DOI: 10.1016/j.ijheatmasstransfer.2010.11.039

Hussain, S., Mehmood, K., & Sagheer, M. (2016). MHD mixed convection and entropy generation of water-alumina nanofluid flow in a double lid driven cavity with discrete heating. *Journal of Magnetism and Magnetic Materials*, *419*, 140-155. DOI: 10.1016/j.jmmm.2016.06.006

Incropera, F. P., & DeWitt, D. P. (1996). *Introduction to Heat Transfer*. New York, USA: John Wiley & Sons, Inc.

Jeong, J., Li, C., Kwon, Y., Lee, J., Kim, S. H., & Yun, R. (2013). Particle shape effect on the viscosity and thermal conductivity of ZnO nanofluids. *International Journal of Refrigeration*, *36*(8), 2233-2241. DOI: 10.1016/j.ijrefrig.2013.07.024

Karimi, A., Goharkhah, M., Ashjaee, M., & Shafii, M. B. (2015). Thermal conductivity of fe2o3 and fe3o4 magnetic nanofluids under the influence of magnetic field. *International Journal of Thermophysics*, *36*(10), 2720-2739. DOI: 10.1007/s10765-015-1977-1

Keyvani, M., Afrand, M., Toghraie, D., & Reiszadeh, M. (2018). An experimental study on thermal conductivity of cerium oxide/ethylene glycol nanofluid: developing a new correlation. *Journal of Molecular Liquids*, *266*, 211-217. DOI: 10.1016/j.molliq.2018.06.010

Khodadadi, H., Toghraie, D., & Karimipour, A. (2019). Effects of nanoparticles to present a statistical model for the viscosity of MgO-water nanofluid. *Powder Technology*, *342*,166-180. DOI: 10.1016/j.powtec.2018.09.076

Liou, T. M., Wei, T.C., & Wang, C. S. (2019). Investigation of nanofluids on heat transfer enhancement in a louvered microchannel with lattice Boltzmann method. *Journal of Thermal Analysis and Calorimetry*, *135*, 751-762. DOI: 10.1007/s10973-018-7299-3

Meyer, J. P., Adio, S. A., Sharifpur, M., & Nwosu, P. N. (2016). The viscosity of nanofluids: a review of the theoretical, empirical and numerical models. *Heat Transfer Engineering*, *37*(5), 387-421. DOI: 10.1080/01457632.2015.1057447

Rashidi, M. M., Nasiri, M., Khezerloo, M., & Laraqi, N. (2016). Numerical investigation of magnetic field effect on mixed convection heat transfer of nanofluid in a channel with sinusoidal walls. *Journal of Magnetism and Magnetic Materials*, 401, 159-168. DOI: 10.1016/j.jmmm.2015.10.034

Rosensweig, R. E. (1997). *Ferrohydrodynamics*. New York, USA: Dover Publications, Inc.

Sardarabadi, H., Heris, S. Z., Ahmadpour, A., & Passandideh-Fard, M. (2019). Experimental investigation of a novel type of two-phase closed thermosyphon filled with funtionalized carbon nanotubes/water nanofluids for electronic cooling application. *Energy Conversion and Management*, *188*, 321-332. DOI: 10.1016/j.enconman.2019.03.070

Shahsavar, A., Khanmohannadi, S., Toghraie, D., & Salihepour, H. (2019). Experimental investigation and develop ANNs by introducing the suitable architectures and training algorithms supported by sensitivity analysis: Measure thermal conductivity and viscosity for liquid paraffin based nanofluid containing Al_2O_3 nanoparticles. *Journal of Molecular Liquids*, *276*, 850-860. DOI: 10.1016/j.molliq.2018.12.055

Sun, B., Lei, W., & Yang, D. (2015). Flow and convective heat transfer characteristics of Fe2O3-water nanofluids inside copper tubes. *International Communication of Heat and Mass Transfer*, *64*, 21-28. DOI: 10.1016/j.icheatmasstransfer.2015.01.008

Toghraie, D., Abdollah, M. M. D., Pourfattah, F., Akbari, O. A., & Ruhani, B. (2018). Numerical investigation of flow and heat transfer characteristics in smooth, sinusoidal and zigzag-shaped microchannel with and without nanofluid. *Journal of Thermal Analysis and Calorimetry*, *131*(2), 1757-1766. DOI: 10.1007/s10973-017-6624-6

Toghraie, D., Alempour, S. M., & Afrand, M. (2016). Experimental determination of viscosity of water based, magnetic nanofluid for application in heating and cooling systems. *Journal of Magnetism and Magnetic Materials*, *417*, 243-248. DOI: 10.1016/j.jmmm.2016.05.092

Yarahmadi, M., Goudarzi, H. M., & Shafii, M. B. (2015). Experimental investigation into laminar forced convective heat transfer of ferrofluids under constant and oscillating magnetic field with different magnetic field arrangements and oscillation modes. *Experimental Thermal and Fluid Science*, *68*, 601-611. DOI: 10.1016/j.expthermflusci.2015.07.002

Zadeh, A. D., & Toghraie, D. (2018). Experimental investigation for developing a new model for the dynamic viscosity of silver/ethylene glycol nanofluid at different temperatures and solid volume fractions. *Journal of Thermal Analysis and Calorimetry*, *131*(2), 1449-1461. DOI: 10.1007/s10973-017-6696-3

Zhou, J., Gu, G., Meng, X., & Shao, C. (2019). Effect of alternating gradient magnetic field on heat transfer enhancement of magnetorheological fluid flowing through microchannel. *Applied Thermal Engineering*, *150*, 1116-1125. DOI: 10.1016/j.applthermaleng.2019.01.057